Inorganica Chimica Acta 489 (2019) 230–235

Contents lists available at ScienceDirect

Inorganica Chimica Acta

journal homepage: www.elsevier.com/locate/ica

Research paper

Dual action photosensitive platinum(II) anticancer prodrugs with photoreleasable azide ligands

Huayun Shi, Guy J. Clarkson, Peter J. Sadler*

Department of Chemistry, University of Warwick, Coventry CV4 7AL, UK

A B S T R A C T

The synthesis, characterisation and properties of novel photosensitive Pt(II) complexes [Pt(terpyridine)(N_3)]CF_3SO_3 (**1b**·CF_3SO_3) and [Pt(NˆCˆN)(N_3)] (**2b**) containing photoreleasable azide ligands with potential as dual photochemotherapeutic and photodynamic therapeutic agents are reported. Their X-ray crystal structures show distorted square-planar Pt(II) coordination geometry with π-stacking between adjacent planar Pt units. These complexes intercalate into DNA with similar binding ability as their chlorido analogues and generate singlet oxygen upon irradiation with blue light (420 nm). Photoactivation of azido complexes leads to the release of the azide ligands and the formation of new platinum species. These properties appear to be favourable for potential dual-action photoactive prodrugs.

1. Introduction

The introduction of light into cancer therapy providesa new avenue to anticancer drug design to circumvent the problems associated with cisplatin [1–4]. Photodynamic therapy (PDT) and photoactivated chemotherapy (PACT) have proven to be promising new, effective, and non-invasive chemotherapeutic treatment modalities [5–8]. PDT is a clinically approved medical technique used for the treatment of malignant tissues, which is based on the combination of a photosensitizer, light and oxygen. PACT, in contrast, kills cells with the cytotoxic photodecomposition products from the stable non-toxic prodrugs and is less dependent on oxygen.

The planar $[Pt(terpy)X]^+$ complexes (terpy = 2,2′:6′,2″-terpyridine; X = Cl, SR) are regarded as classic DNA metallointercalators [9–12], and their application in anticancer therapy has attracted recent interest [13–16]. Cyclometalated platinum(II) complexes [Pt(tri)X/L] supported by π-conjugated tridentate ligands (tri) have been widely studied due to their stability and intriguing photophysical properties [14–19]. Notably, some studies have demonstrated their potential as photosensitizers that can generate reactive oxygen species (ROS) upon irradiation and exhibit photocytotoxicity towards cancer cells [20–22].

Azide ligands are key components in second generation photoactive platinum(IV) complexes [1–4,23–25]. Azidyl radicals can be released from the platinum centres and attack cancer cells [26]. In early examples, two azide ligands on the same platinum centre appeared to be necessary for the photodecomposition, each donating one electron leading to photoreduction of Pt(IV) to Pt(II) [27]. However, in some systems only a single azide ligand appeared to be active in the initial photoreduction [28,29].

Platinum complexes bearing terpyridine or NˆCˆN pincer type ligands offer a planar scaffold to intercalate into DNA and can be used in PDT, whilst the introduction of azide ligands can allow photoactivation. Herein, we have synthesised two platinum complexes [Pt(terpyridine)(N_3)]CF_3SO_3 (**1b**·CF_3SO_3) and [Pt(NˆCˆN)(N_3)] (NˆCHˆN = 1,3-di(pyridin-2-yl)benzene, **2b**) containing both pincer and azide ligands (Scheme 1). The X-ray crystal structures of complexes **1b**·CF_3SO_3 and **2b** were determined, and their photophysical properties, photodecomposition, singlet oxygen production, and DNA binding have been studied. We envisaged that these complexes might behave as dual PDT and PACT agents and have potential for selective photocytotoxicity.

2. Experimental section

2.1. Materials and instruments

All chemicals were purchased from Sigma Aldrich and used without further purification. NMR spectra were recorded on Bruker Avance III HD 300 or 400 MHz spectrometers with the residual signal of the solvent used as a reference. ESI-MS spectra were recorded on an Agilent 6130B single quadrupole detector instrument. Electronic absorption spectra were recorded on a Varian Cary 300 UV–vis spectrophotometer in a quartz cuvette and referenced to neat solvent. Fluorescence spectra were obtained on a Jasco FP-6500 spectrofluorometer. The emission quantum yields were measured using $[Ru(bpy)_3]Cl_2$ in acetonitrile as standard [30] (Φ_r = 0.018, excitation wavelength at 450 nm) and calculated from $\Phi_{em} = \Phi_r\ (B_r/B_s)(n_s/n_r)^2(D_s/D_r)$, where the subscripts s and r refer to sample and reference standard, respectively, n is the refractive index of the solvents, D is the integrated intensity, and Φ is the

* Corresponding author.
E-mail address: p.j.sadler@warwick.ac.uk (P.J. Sadler).

https://doi.org/10.1016/j.ica.2019.02.016
Received 7 December 2018; Received in revised form 14 February 2019; Accepted 17 February 2019
Available online 18 February 2019
0020-1693/

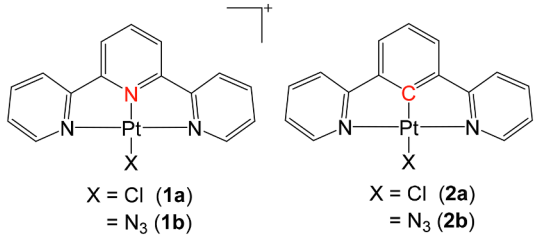

Scheme 1. The chemical structures of the platinum(II) complexes studied in this work.

luminescence quantum yield. The quantity B is calculated from $B = 1-10^{-AL}$, where A is the absorbance at the excitation wavelength and L is the optical path length. Analytical reversed-phase HPLC analyses were carried out on an Agilent ZORBAX Eclipse XDB-C18 column (250 × 4.6 mm, 5 µm, flow rate: 1 mL/min), by using linear gradients of 0.1% v/v TFA in H_2O (solvent A) and 0.1% v/v TFA in CH_3CN (solvent B). LC-MS was carried out on a Bruker Amazon X instrument connected online with HPLC. The light source used for photoactivation was a LZC-ICH2 photoreactor (Luzchem Research Inc.) equipped with a temperature controller and 8 Luzchem LZC-420 lamps without light filtration.

2.2. Synthesis and characterization

Caution! Heavy metal azides can be shock-sensitive detonators. We did not encounter any problems during the work reported here but due care and attention with appropriate precautions should be taken in their synthesis and handling.

All syntheses and purifications were carried out in the dark with minimal light exposure.

General synthetic procedure for complexes **1b**·CF_3SO_3 and **2b**

A mixture of the corresponding parent chlorido complexes (25 mg) and 10 mol equiv of sodium azide in anhydrous DMF (2 mL) was stirred at 338 K for 24 h. After evaporation to dryness, the residue was washed with water and diethyl ether. Recrystallization was carried out by diffusion of ether into the DCM solution of crude product.

1b·CF_3SO_3: ^{1}H NMR (DMSO-d_6, 300 MHz): 8.71–8.53 (m, 9H), 8.04 (t, J = 6.3 Hz, 2H). ESI-MS [M^+]: 470.4. Anal. Calcd: $C_{16}H_{11}N_6O_3F_3SPt$: C 31.02, H 1.79, N 13.57. Found: C 31.23, H 1.75, N 13.25.

2b: ^{1}H NMR ($CDCl_3$, 400 MHz): 8.83 (d with satellites, J = 5.6 Hz, J ^{195}Pt-^{1}H = 40.7 Hz, 2H), 7.96 (t, J = 7.8 Hz, 2H), 7.70 (d, J = 7.9 Hz, 2H), 7.41 (d, J = 7.7 Hz, 2H), 7.32 (t, J = 6.5 Hz, 2H), 7.17 (t, J = 7.7 Hz, 1H). ESI-MS [M + Na^+]: 491.4. Anal. Calcd: $C_{16}H_{11}N_5Pt$: C 41.03, H 2.37, N 14.95. Found: C 40.86, H 2.22, N 14.75.

2.3. X-Ray crystallography

Single crystals of **1b**·CF_3SO_3 and **2b** were grown from DCM/ether at room temperature. A suitable crystal was selected and mounted on a Mitegen head with Fomblin oil and placed on an Xcalibur Gemini diffractometer with a Ruby CCD area detector. The crystal was kept at 150(2) K during data collection. Using Olex2 [31], the structure was solved with the ShelXT [32] structure solution program using Direct Methods and refined with the ShelXL [33] refinement package using Least Squares minimisation.

2.4. DNA binding studies

For a typical UV − vis and emission titration experiment, aliquots of a millimolar stock *ct*-DNA (base concentration = 2.4 mM) were added to a solution of the complex (24 µM, 3 mL) in PBS by a micropipette, and the spectral changes were recorded on Varian Cary 300 UV–vis and Jasco FP-6500 fluorescence spectrophotometers in a quartz cuvette at 298 K. The volume changes after the addition of DNA were kept < 5% (150 µL). The intrinsic binding constant K, was determined from a plot of $D/\Delta\varepsilon_{ap}$ vs D according to Eq. (1):[34,35]

$$D/\Delta\varepsilon_{ap} = D/\Delta\varepsilon + 1/(\Delta\varepsilon \times K) \quad (1)$$

where D is the concentration of DNA, $\Delta\varepsilon_{ap} = |\varepsilon_A - \varepsilon_F|$, $\varepsilon_A = A_{obs}/$[complex], and $\Delta\varepsilon = |\varepsilon_B - \varepsilon_F|$; ε_B and ε_F correspond to the extinction coefficients of DNA − complex adduct and unbound complex, respectively.

2.5. Singlet oxygen measurements by UV–vis spectroscopy

An air-saturated PBS buffer solution, containing the complexes (A = 0.02 at irradiation wavelength), p-nitrosodimethyl aniline (RNO, 20 µM), and histidine (10 mM), was irradiated in a quartz cuvette at 420 nm in a LZC-ICH2 photoreactor (Luzchem Research Inc.) equipped with a temperature controller and 8 Luzchem LZC-420 lamps without light filtration, at different time intervals. The absorbance of the solution was then recorded. Plots of variations in absorbance at 440 nm in PBS versus the irradiation times for each sample were prepared and the slope of the linear regression was calculated (S_{sample}).

Phenalenone ($\Phi_{ref}(^1O_2)$ = 95%) was used as a reference compound [36] in Eq. (2) to calculate the singlet oxygen quantum yield (Φ_{sample}) for every sample:

$$\Phi_{sample} = \Phi_{ref} \times S_{sample}/S_{ref} \times I_{ref}/I_{sample} \quad (2)$$

$$I = I_0 * (1 - 10^{-A_\lambda}) \quad (3)$$

I (absorbance correction factor) was obtained with Eq. (3), where I_0 is the light intensity of the irradiation source and A_λ is the absorbance of the sample at wavelength λ.

3. Results and discussion

3.1. Synthesis and characterisation

Ligand **L2**, and complexes **1a** and **2a** were prepared according to reported methods [37–39]. Their azido analogues **1b** and **2b** were synthesized by stirring the corresponding chlorido complex with 10 mol equiv of sodium azide in DMF at 338 K overnight. The synthesis of [Pt(terpyridine)(N_3)]PF_6 was reported previously using a different method [41]. All complexes are air stable at ambient temperature in the solid state. They gave satisfactory elemental analysis and were further characterized by ESI-MS, NMR, UV–vis and fluorescence spectroscopy, and for complexes **1b**·CF_3SO_3 and **2b** by single crystal X-ray diffraction. The ^{1}H NMR spectra of complexes **1b** and **2b** contain the anticipated peaks, all located at 9.00–7.00 ppm and assignable to aromatic protons (Figures S1 and S2, Supplementary Data file).

3.2. X-ray crystallography

Crystals of complexes **1b**·CF_3SO_3 and **2b** suitable for X-ray diffraction studies were obtained through the diffusion of diethyl ether into corresponding DCM solutions. The crystallographic data are summarized in Table S1 (Supplementary Data file) and selected bond distances and angles are listed in Table 1. Perspective drawings of complexes **1b**·CF_3SO_3 and **2b** are shown in Fig. 1. Complex **1b**·CF_3SO_3 crystallized in the monoclinic space group $P2_1/c$ with a platinum azide complex and associated triflate counter ion in the asymmetric unit. There are four complexes in the unit cell. Neutral complex **2b** crystallized in the triclinic space group P-1 with two complexes in the unit cell related by an inversion centre. The Pt(II) coordination geometry in these complexes is distorted square-planar. The Pt–N bond distances between Pt and auxiliary ligand are in the range of 1.923(2)–2.0388(19) Å, and resemble reported chlorido analogues [38,39]. The Pt–C bond distance is

Table 1
Selected Bond Lengths (Å) and Bond Angles (°) for **1b**·SO_3CF_3 and **2b**.

1b·SO_3CF_3		**2b**	
Pt1···Pt1	3.68	Pt1···Pt1	4.132/4.922
Pt1–N1	2.031(3)	Pt1–N1	2.0309(19)
Pt1–N7	1.923(2)	Pt1–N2	2.118(2)
Pt1–N17	2.021(2)	Pt1–C12	1.910(2)
Pt1–N18	2.019(3)	Pt1–N18	2.0388(19)
N7–Pt1–N18	174.12(10)	C12–Pt1–N2	173.76(9)
N19–N18–Pt1	125.6(2)	N3–N2–Pt1	130.00(19)
N20–N19–N18	176.5(3)	N4–N3–N2	176.3(3)

1.910(2) Å in **2b**. The bound azide N is in a slightly twisted line with Pt and its *trans* N or C, forming an angle of ca. 170°. The azide ligands are almost linear and the Pt–N(α)–N(β) angles are > 120°. For the cation in **1b**, the azide ligand is in the same plane as the auxiliary ligand and Pt, while complex **2b** contains an azide ligand at an angle of 130.00(19)° to the distorted square plane of the auxiliary ligand and Pt.

The cations of **1b** form infinite stacks by π-stacking along the *c* axis of the cell (Figure S3, Supplementary Data file). The angle between mean planes defined by the ligand atoms, the Pt and the N(α) of the azide is 3.042° and closest atomic contact C5···C4′ is 3.382 Å. The adjacent Pt atoms are in a zigzag arrangement with a Pt···Pt···Pt angle of 136.52° and Pt···Pt distance of 3.68 Å. Molecule **2b** forms a dimer-like arrangement (Figure S4, Supplementary Data file), which are π-stacked with a closest atomic contact C3···C13′ of 3.312 Å and adjacent Pt···Pt distance of 4.132 Å. There is further π stacking between these dimers that are more offset with closest atomic contact Pt1···C13′ of 3.407 Å and adjacent Pt···Pt distance of 4.922 Å.

3.3. Photophysical properties

The photophysical data for complexes **1b** and **2b** in aqueous and acetonitrile solutions are summarized in Table S2 (Supplementary Data file) together with those of complexes **1a** and **2a** for comparison. The spectra of complexes **1a** and **2a** match well with those reported [40,41]. As shown in Fig. 2a and S5a (Supplementary Data file), complexes **1b** and **2b** exhibit a set of intense bands in the UV region (λ < 360 nm), which can be assigned as intraligand (IL) [π - π*] transitions of the cyclometalated NˆCˆN or NˆNˆN ligands. The low-energy absorption bands are tentatively assigned as a mixture of IL transitions of the cyclometalated ligand and metal-to-ligand charge-transfer (MLCT) transitions. A hyperchromic and red-shifted absorption band is observed for complexes **1b** and **2b** when compared with their chlorido analogues, which might be assignable as LMCT involving Pt(II) and N_3.

Excitation of complex **2b** at λ > 380 nm in aqueous or acetonitrile solution resulted in long-lived and intense emission of green light at 298 K, with quantum yields Φ = 0.026 in PBS and = 0.038 in acetonitrile (Fig. 2b, Figure S5b and Table S2, Supplementary Data file). However, the fluorescence of **1b** was too weak to be measured. Complex **2b** exhibits well-resolved vibronic-structured emission bands at ca. 480–600 nm with progressional vibrational spacings of *ca.* 1150 cm^{-1} in acetonitrile and *ca.*1300–1450 cm^{-1} in PBS. The parent chlorido complexes have similar emission spectra as the corresponding azido analogues, except for higher quantum yield and relatively less intense emission in the yellow region (550–600 nm).

3.4. Photodecomposition of azido complexes

Upon irradiation with blue light (420 nm), azido complexes **1b** and **2b** underwent decomposition in PBS and acetonitrile solutions at ambient temperature. Fig. 3b for acetonitrile, shows an apparent decrease in absorption peaks of complex **1b** at ca. 324, 338, and 427 nm, accompanied by the appearance of new absorption bands at 246, 275, 327, and 340 nm, attributable to the release of the azide ligands. The change is less significant in PBS. Decreases in absorbance at 278, 327 and 344 nm were observed (Figure S6b, Supplementary Data file). However, no noticeable spectral change was found for the chlorido complex **1a** in either PBS or acetonitrile (Figs. 3a and S6a, Supplementary Data file). Similar results were obtained for complexes **2a** and **2b** in acetonitrile. However, due to the relatively lower aqueous solubility and the potential to form aggregate due to π stacking of complexes **2a** and **2b**, their UV–vis spectra suggested that they are not so stable in PBS. Therefore, LC-MS was employed to investigate the products from photoactivation of azido complex **2b** in PBS solution. A single peak assigned as **2b** was observed before irradiation. An unidentified new peak assignable to platinum complex that might contain chloride (m/Z = 497.12) appeared after 1 h irradiation of blue light (Figure S7, Supplementary Data file).

LC-MS studies based on the photodecomposition of azido complexes **1b** and **2b** in ACN were carried out to investigate the decomposition pathway (Figure S8, Supplementary Data file). For both of complexes, the platinum(II) species generated from the release of azide ligand ([{Pt(terpyridine)(OH)} + H_2O]$^+$ (462.97) and {Pt(terpyridine)(HCOO)}$^+$ (472.98) for **1b**, [2{Pt(NˆCˆN)(OH)} + H_3O]$^+$ (905.12) for **2b**) were detected after 1 h irradiation with blue light. However, released tridentate ligand was observed for **2b** after irradiation, while not found for **1b**. In comparison, the chlorido complexes were stable towards light.

3.5. Singlet oxygen generation

Singlet oxygen $^1O_2$ is the key active species in killing cancer cells using photodynamic therapy [42]. In this work, we used an indirect method to determine the photosensitization of molecular oxygen. This method involved monitoring the absorbance of a probe molecule for

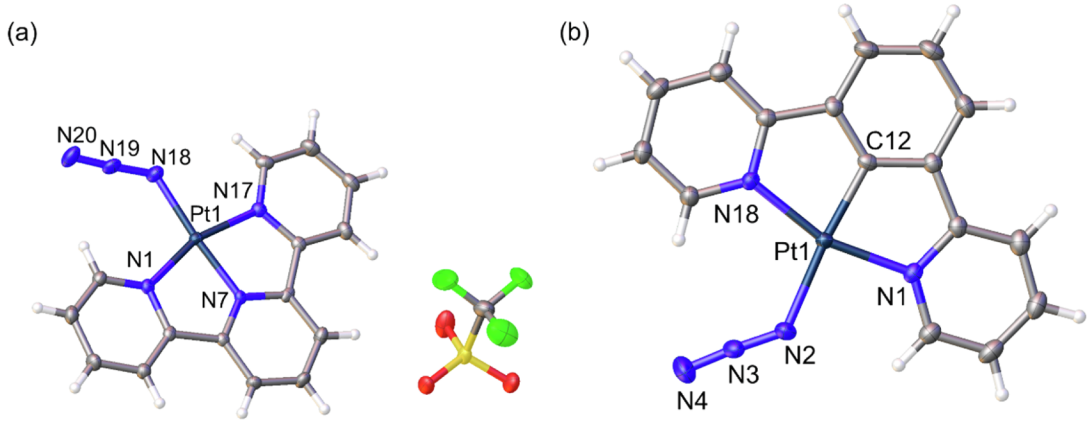

Fig. 1. X-ray crystal structures of (a) **1b**·SO_3CF_3, and (b) **2b**, with key atom labels, and thermal ellipsoids drawn at 50% probability level.

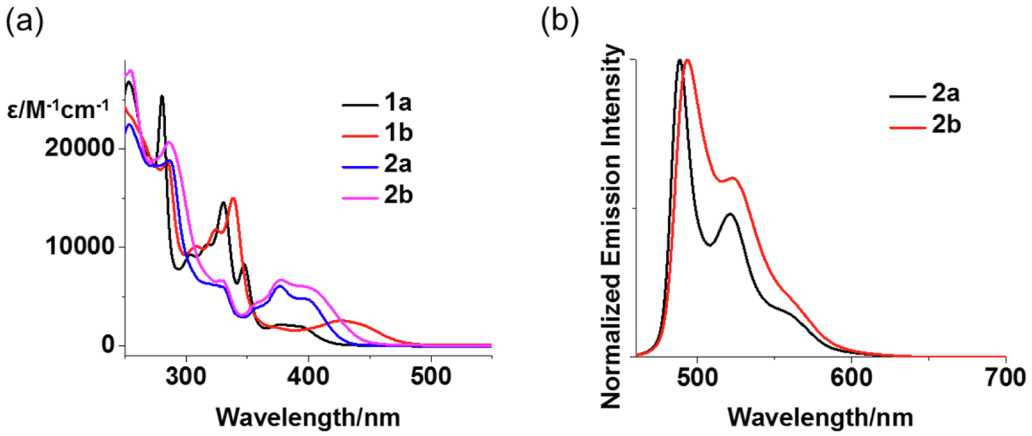

Fig. 2. (a) UV–vis absorption spectra, and (b) emission spectra of the platinum(II) complexes in acetonitrile.

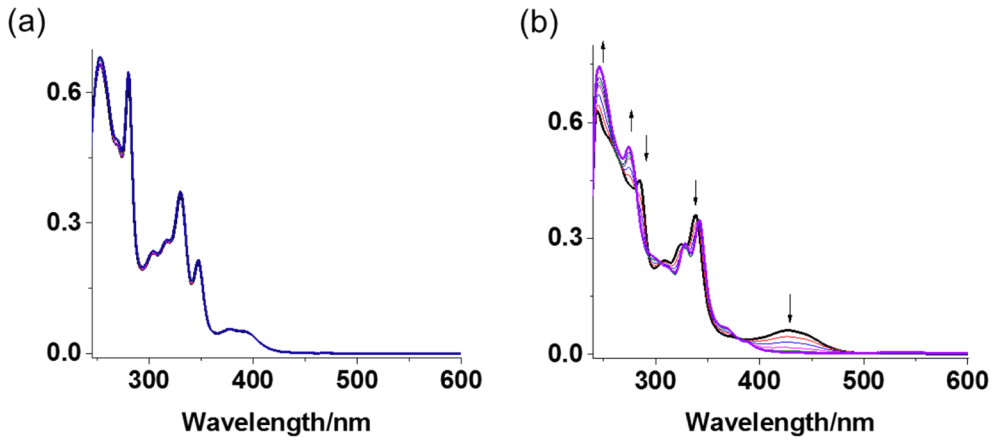

Fig. 3. (a) Photochemical decomposition of complex **1a**, and (b) complex **1b** in acetonitrile upon irradiation with blue light (420 nm) for 1 h.

Table 2
Singlet oxygen quantum yields of platinium(II) complexes **1a** and **1b**, **2a** and **2b** in PBS with 420 nm excitation.

Complex	$\Phi(^1O_2)$ at 420 nm/%[a]
1a	9.6
1b	19.4
2a	9.9
2b	13.8

[a] Phenalenone was used as reference [36].

Table 3
DNA-binding constants *K* for complexes **1a** and **2a**, **1b** and **2b** in PBS.

Complex	Binding constant/M^{-1}
1a	4.34×10^3
1b	5.02×10^3
2a	2.63×10^4
2b	2.15×10^4

$^1O_2$. Generated $^1O_2$ can react with histidine in PBS and quench the absorbance of the probe molecule, p-nitrosodimethyl aniline (RNO). Phenalenone was used as a reference (quantum yield 95%) [36].

The measured values for complexes **1b** and **2b** in PBS are listed in Table 2 with chlorido complexes **1a** and **2a** for comparison. Even though the singlet oxygen quantum yields for all of the complexes are not promising in PBS (< 20%), those for azido complexes are 1.4–2.0 × higher than their chlorido analogues (Figure S9, Supplementary Data file). The spectral change caused by photodecomposition has been allowed for in the calculation of the singlet oxygen quantum yield. The low quantum yields might be caused by the fast interaction between the auxiliary ligand and H_2O, which quenches the excited state and inhibits energy transfer to oxygen.

3.6. DNA binding studies

Planar $[Pt(L)X]^{0/+}$ (L = NˆCˆN or NˆNˆN) complexes are classical DNA metallointercalators. The DNA binding ability of photosensitizers can allow them to generate $^1O_2$ close to DNA, and thus oxidize genetic material efficiently. The binding to *ct*-DNA was investigated by absorption spectroscopy titrations (Table 3). Fig. 4b shows the spectral change of **2b** upon addition of DNA. The intense absorption band at *ca.* 320 and 390 nm decreased in intensity with increasing DNA concentration, characteristic of an intercalative interaction [13]. The binding constant was determined to be 2.15×10^4 M^{-1} using the Scatchard equation [34,35], and comparable with the chlorido analogue **2a** (2.63×10^4 M^{-1}, Fig. 4a). Complexes **1a** and **1b** showed similar spectral change upon DNA titration in PBS, although the binding constants are smaller.

Complex **2b** exhibits intense fluorescence in PBS, which was further enhanced in the presence of DNA (Fig. 5) up to a [DNA]/[**2b**] ratio of 10. The plot of I/I_o vs. [DNA]/[**2b**] (I and I_o are emission intensities of platinum complexes with and without DNA), shows a DNA-induced enhancement of 5.5-fold. A similar spectral change was observed for complex **2a**, which matches the reported results.[43]

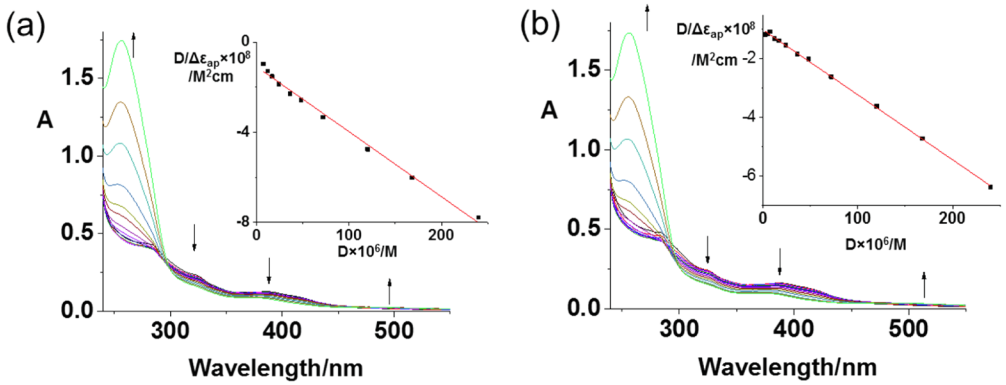

Fig. 4. (a) UV-vis spectral changes for complexes **2a**, and (b) **2b** (24.0 μM) in PBS buffer solution with increasing ratio of [DNA]/[Pt] = 0–10 at 298 K. Insert: Linear plots for the determination of the intrinsic binding constant *K*.

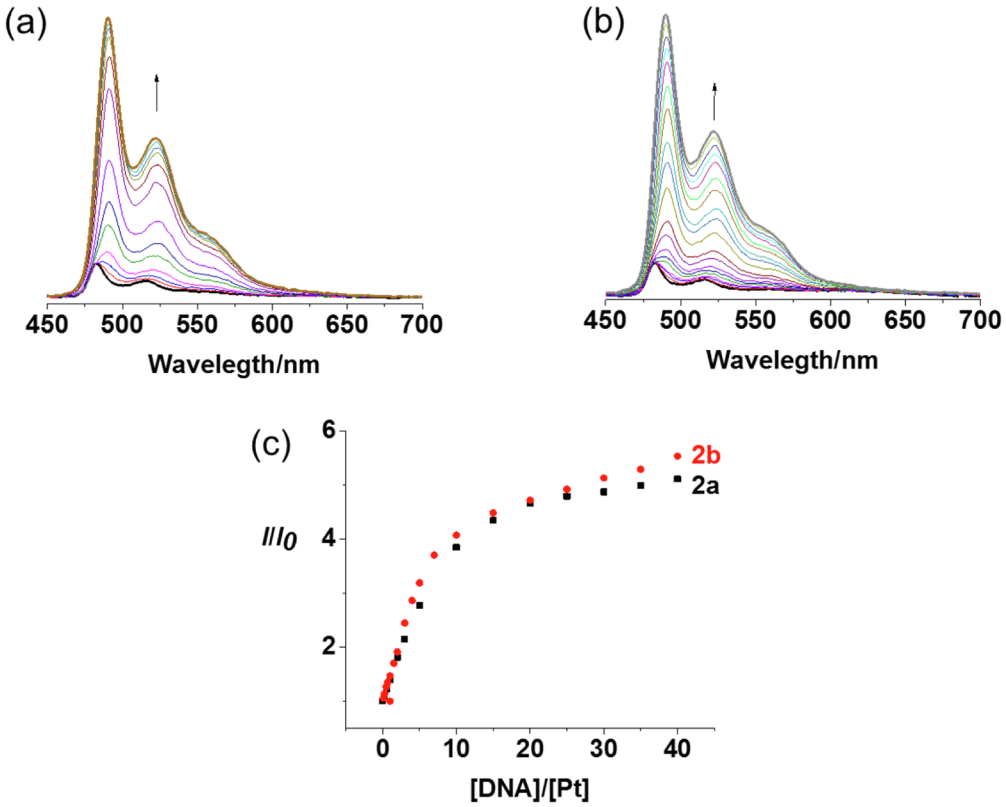

Fig. 5. (a) Fluorescence spectral change for complexes **2a**, and (b) **2b** in PBS buffer solution (24.0 μM) with increasing ratio of [DNA]/[Pt] = 0–40 at 298 K. (c) Plot of I/I_0 vs [DNA]/[Pt] for the emission titration study of the complex-DNA interaction.

4. Conclusions

In conclusion, square-planar platinum(II) complexes containing a π-conjugated pincer ligand and a monodentate azide ligand have been synthesised and characterised, including their X-ray crystal structures. Their $\{Pt(terpy)\}^+$ and $\{Pt(N^{\wedge}C^{\wedge}N)\}^+$ fragments play a critical role in intercalation into DNA and production of singlet oxygen upon photo-activation, while azide can act as a leaving ligand. This strategy of combining a PACT prodrug and PDT photosensitizer, has the potential in improving both the photocytotoxicity and photoselectivity.

Acknowledgements

This research was supported by the EPSRC (grants EP/G006792, EP/F034210/1 to PJS), ERC (grant 247450 to PJS), and a Chancellor's International PhD Scholarship from the University of Warwick (for HS).

Appendix A. Supplementary data

Supplementary data to this article can be found online at https://doi.org/10.1016/j.ica.2019.02.016.

References

[1] K. Mitra, Dalton Trans. 45 (2016) 19157.
[2] S.J. Berners-Price, Angew. Chem. Int. Ed. 50 (2011) 804.
[3] N.A. Smith, P.J. Sadler, Phil. Trans. R Soc. A 371 (2013) 20120519.
[4] A. Bjelosevica, B.J. Pagesa, L.K. Sparea, K.M. Deoa, D.L. Ang, J.R. Aldrich-Wrighta, Curr. Med. Chem. 25 (2018) 478.
[5] D.E.J.G.J. Dolmans, D. Fukumura, R.K. Jain, Nat. Rev. Cancer 3 (2003) 380.
[6] P.J. Bednarski, F.S. Mackay, P.J. Sadler, Anti-Cancer Agents Med. Chem. 7 (2007) 75.

[7] M.C. DeRosa, R.J. Crutchley, Coord. Chem. Rev. 233 (2002) 351.
[8] F. Heinemann, J. Karges, G. Gasser, Acc. Chem. Res. 50 (2017) 2727.
[9] K.W. Jennette, S.J. Lippard, G.A. Vassiliades, W.R. Bauer, Proc. Natl. Acad. Sci. USA 71 (1974) 3839.
[10] M.H. Grant, K.C. Wu, W.R. Bauer, S.J. Lippard, Biochemistry 15 (1976) 4339.
[11] S.J. Lippard, Acc. Chem. Res. 11 (1978) 211.
[12] G. Lowe, A.S. Droz, T. Vilaivan, G.W. Weaver, L. Tweedale, J.M. Pratt, P. Rock, V. Yardley, S.L. Croft, J. Med. Chem. 42 (1999) 999.
[13] D.L. Ma, T.Y.T. Shum, F. Zhang, C.M. Che, M. Yang, Chem. Commun. (2005) 4675.
[14] P. Wang, C.H. Leung, D.L. Ma, W. Lu, C.M. Che, Chem. Asian J. 5 (2010) 2271.
[15] K. Li, T. Zou, Y. Chen, X. Guan, C.M. Che, Chem. Eur. J. 21 (2015) 7441.
[16] S.K. Fung, T. Zou, B. Cao, T. Chen, W.P. To, C. Yang, C.N. Lok, C.M. Che, Nat. Commun. 7 (2016) 10655.
[17] X.S. Xiao, W.L. Kwong, X. Guan, C. Yang, W. Lu, C.M. Che, Chem. Eur. J. 19 (2013) 9457.
[18] T. Zou, J. Liu, C.T. Lum, C. Ma, R.C.T. Chan, C.N. Lok, W.M. Kwok, C.M. Che, Angew. Chem. Int. Ed. 53 (2014) 10119.
[19] R.W.Y. Sun, A.L.F. Chow, X.H. Li, J.J. Yan, S.S.Y. Chui, C.M. Che, Chem. Eur. J. 19 (2013) 9457.
[20] K. Mitra, U. Basu, I. Khan, B. Maity, P. Kondaiah, A.R. Chakravarty, Dalton Trans. 43 (2014) 751.
[21] K. Mitra, A. Shettar, P. Kondaiah, A.R. Chakravarty, Inorg. Chem. 55 (2016) 5612.
[22] R.E. Doherty, I.V. Sazanovich, L.K. McKenzie, A.S. Stasheuski, R. Coyle, E. Baggaley, S. Bottomley, J.A. Weinstein, H.E. Bryant, Sci. Rep. 6 (2016) 22668.
[23] P. Müller, B. Schröder, J.A. Parkinson, N.A. Kratochwil, R.A. Coxall, A. Parkin, S. Parsons, P.J. Sadler, Angew. Chem. Int. Ed. 42 (2003) 335.
[24] F.S. Mackay, J.A. Woods, P. Heringová, J. Kašpárková, A.M. Pizarro, S.A. Moggach, S. Parsons, V. Brabec, P.J. Sadler, Proc. Natl. Acad. Sci. USA 104 (2007) 20743.
[25] N.J. Farrer, J.A. Woods, L. Salassa, Y. Zhao, K.S. Robinson, G. Clarkson, F.S. Mackay, P.J. Sadler, Angew. Chem. Int. Ed. 49 (2010) 8905.
[26] J.S. Butler, J.A. Woods, N.J. Farrer, M.E. Newton, P.J. Sadler, J. Am. Chem. Soc. 134 (2012) 16508.
[27] A. Vogler, A. Kern, Angew. Chem. Int. Ed. 17 (1978) 524.
[28] H.I.A. Phillips, L. Ronconi, P.J. Sadler, Chem. Eur. J. 15 (2009) 1588.
[29] L. Salassa, H.I.A. Phillips, P.J. Sadler, Phys. Chem. Chem. Phys. 11 (2009) 10311.
[30] K. Suzuki, A. Kobayashi, S. Kaneko, K. Takehira, T. Yoshihara, H. Ishida, Y. Shiina, S. Oishic, S. Tobita, Phys. Chem. Chem. Phys. 11 (2009) 9850.
[31] O.V. Dolomanov, L.J. Bourhis, R.J. Gildea, J.A.K. Howard, H. Puschmann, J. Appl. Cryst. 42 (2009) 339.
[32] G.M. Sheldrick, Acta Cryst. A71 (2015) 3.
[33] G.M. Sheldrick, Acta Cryst. C71 (2015) 3.
[34] D.E.V. Schmechel, D.M. Crothers, Biopolymers 10 (1971) 465.
[35] A. Wolfe, G.H. Shimer, T. Meehan, Biochemistry 26 (1987) 6392.
[36] R. Schmidt, C. Tanielian, R. Dunsbach, C. Wolff, J. Photochem. Photobiol. A 79 (1994) 11.
[37] C. Liu, N. Han, X. Song, J. Qiu, Eur. J. Org. Chem. (2010) 5548.
[38] S.W. Lai, M.C.W. Chan, K.K. Cheung, C.M. Che, Inorg. Chem. 38 (1999) 4262.
[39] D.J. Cárdenas, A.M. Echavarren, M.C.R. de Arellano, Organometallics 18 (1999) 3337.
[40] H.K. Yip, L.K. Cheng, K.K. Cheung, C.M. Che, J. Chem. Soc. Dalton Trans. (1993) 2933.
[41] W.A. Tarran, G.R. Freeman, L. Murphy, A.M. Benham, R. Kataky, J.A.G. Williams, Inorg. Chem. 53 (2014) 5738.
[42] C. Mari, V. Pierroz, R. Rubbiani, M. Patra, J. Hess, B. Spingler, L. Oehninger, J. Schur, I. Ott, L. Salassa, S. Ferrari, G. Gasser, Chem. Eur. J. 20 (2014) 14421.
[43] D.A.K. Vezzu, Q. Lu, Y.H. Chen, S. Huo, J. Inorg. Biochem. 134 (2014) 49.